Expert Systems
The Journal of Knowledge Engineering

Article

DOI: 10.1111/j.1468-0394.2009.00488.x

Fuzzy sliding mode control of a finger of a humanoid robot hand

Yunus Ziya Arslan, Yuksel Hacioglu and Nurkan Yagiz
Department of Mechanical Engineering, Faculty of Engineering, Istanbul University, 34320 Avcilar, Istanbul, Turkey
Email: nurkany@istanbul.edu.tr

Abstract: *The motion control problem for the finger of a humanoid robot hand is investigated. First, the index finger of the human hand is dynamically modelled as a kinematic chain of cylindrical links. During construction of the model, special attention is given to determining bone dimensions and masses that are similar to the real human hand. After the kinematic and dynamic analysis of the model, in order to ensure that the finger model tracks its desired trajectory during a closing motion, a fuzzy sliding mode controller is applied to the finger model. In this controller, a fuzzy logic algorithm is used in order to tune the control gain of the sliding mode controller; thus, an adaptive controller is obtained. Finally, numerical results, which include a performance comparison of the proposed fuzzy sliding mode controller and a conventional sliding mode controller, are presented. The results demonstrate that the proposed control method can be used to perform the desired motion task for humanoid robot hands efficiently.*

Keywords: humanoid robot hand finger, fuzzy sliding mode control, dynamic analysis

1. Introduction

Dextrous humanoid robot hands have been developed in the last few decades, e.g. the Belgrade/USC Hand, the Stanford/JPL Hand, the Utah/MIT Dextrous Hand and the DLR Hand etc. (Jacobsen *et al.*, 1986; Hirzinger *et al.*, 2000; Banks, 2001). The need for improving the dextrous robot hands and end-effectors arises from the desire to adapt the motion mechanisms of the human hand to robotic and prosthetic hand designs in order to mimic natural movements and handle objects of different sizes and shapes like human hands (Li *et al.*, 2000; Pollard & Gilbert, 2002). Therefore, to design robot hands that have human-like qualities, the human hand should be investigated from the viewpoint of biomechanics.

The human hand is a very articulated structure and it can be considered as a linkage system of intercalated bony segments. Many biomechanical models of the human hand have been developed (Armstrong & Chaffin, 1978; An *et al.*, 1979; Buchholz & Armstrong, 1992; Miller *et al.*, 2005). Anthropometric data and limitations of motion capabilities of the human hand can be derived from these studies. Furthermore, many investigators have suggested various biomechanical models for the human hand fingers and they have carried out studies to determine the kinematic and dynamic behaviours of the fingers (Youm *et al.*, 1978; Buchner *et al.*, 1988; Brook *et al.*, 1995; Biggs & Horch, 1999; Vigouroux *et al.*, 2006). Additionally, the fundamental neuro-musculo-skeletal components of fingers and their interactions have also been investigated to analyse the biomechanical function and neuromuscular control of the fingers (Valero-Cuevas, 2005). Excluding the thumb, the kinematic structures of the finger bones are

© 2009 The Authors. Journal Compilation © 2009 Blackwell Publishing Ltd

similar to each other. Therefore, motion analysis of only one finger provides a general evaluation of the whole human hand behaviour.

Proportional-integral-derivative (PID) controllers are widely used in industrial applications. On the other hand, this type of control is not efficient when there are parameter variations and external disturbances. Therefore fuzzy PID control was introduced to deal with parameter variations. Kazemian (2005) presented a novel self-organizing fuzzy PID controller in which the PID gains are tuned at a supervisory level using fuzzy logic. His paper concludes that the fuzzy PID controller produces a better output response than the classical PID controller. Sliding mode control, as a robust and special class of variable structure, is preferred in robotics and in a variety of applications because of its invariance properties. This control method became widespread after a paper by Utkin (1977). The basic idea of the method is to drive the system states to the so-called sliding surface and then keep the system within a neighbourhood of this surface. Slotine and Sastry (1983) developed a sliding mode controller for control of time-varying non-linear systems and applied this controller to a two-link manipulator, for handling variable loads in a flexible manufacturing system environment. Gao and Hung (1993) presented a new approach, called the reaching law method, for the design of a variable structure controller for non-linear systems. The approach was applied to a two-link robot arm to demonstrate its effectiveness. Cavallo and Natale (2004) proposed a control strategy based on a second-order sliding manifold multiple-input multiple-output approach, which is used to design a robust multivariable linear controller. A manipulator with 6 degrees of freedom (df) was used as a test bed for experiments. Herman (2005) presented a sliding mode controller for a rigid manipulator in terms of the generalized velocity components vector, and tested this control method on a 3 df robot.

In recent years, great effort has been made in order to improve the transient performance of the sliding mode controller. Much work has focused on the time-varying sliding surface design, where the surface can rotate or shift in a prescribed manner (Choi *et al.*, 1993; Bartoszewicz, 1995; Tokat, 2006). A fuzzy tuning scheme for the sliding surface rotation has also been presented (Ha *et al.*, 1999). In addition to these studies, fuzzy logic algorithms for tuning the control gain of the sliding mode controller were presented (Guo & Woo, 2003; Lin & Mon, 2003), since the control gain has a direct effect on the reaching phase. Therefore a fuzzy logic algorithm for adaptation of the control gain of the sliding mode controller is presented in this study.

The main objective of this study is to analyse the kinematics, dynamics and control of the closing motion of the finger of a humanoid robot hand. The remainder of the paper is organized as follows. After a brief introduction to the anatomy of the human hand in Section 2, a dynamic model of the finger, which is based on an approximate model of human hand anatomy, is presented in Section 3. During the construction of the model, care was taken to ensure that the bone dimensions and masses are similar to a real human hand. Then, the robust fuzzy sliding mode control method is presented and applied to this finger model to track the trajectory, which is determined by using camera images of a real human hand. Finally, numerical results for the finger of a humanoid robot hand during the closing motion are presented in the last section.

2. Human hand anatomy

The human hand has an articulated structure having high functionality which is based on its multiple degrees of freedom. The human hand has 23 df provided by 17 joints (LaViola, 1999). If spatial motion is taken into consideration, the degrees of freedom increase to 29 because of orientation and position variation of the hand. In Figure 1, the skeletal structure of the hand which demonstrates the degrees of freedom of the joints is depicted.

The finger skeleton consists of bone segments called phalanges. The nearest phalange to the palm is called the proximal phalange and the

 © 2009 The Authors. Journal Compilation © 2009 Blackwell Publishing Ltd

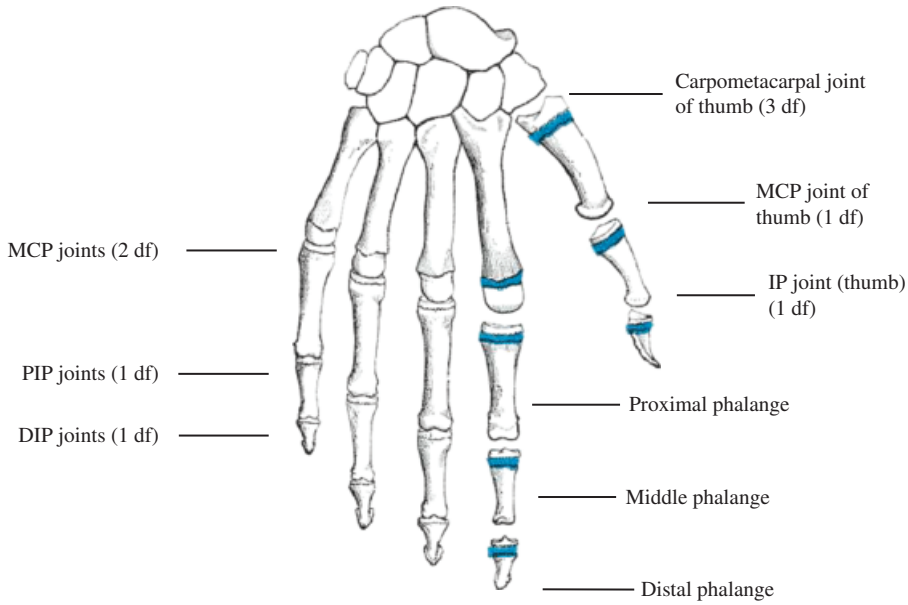

Figure 1: *Skeletal structure of the human hand (Gray, 1858).*

one at the end of each finger is called the distal phalange. The distal interphalangeal (DIP) and proximal interphalangeal (PIP) joints have 1 df owing to rotational motion and the metacarpophalangeal (MCP) joint has 2 df owing to adduction/abduction and rotational motions. The index, middle, ring and little fingers of the hand have similar structure in terms of kinematic and dynamic features. The thumb has the most complex physical structure amongst the fingers and requires an extra effort during modelling because the metacarpal segment of the thumb is a part of both thumb and palm (de Campos, 2006). The index finger has the greatest range of motion amongst the fingers such that, for the extension/flexion movement, the maximum dynamic range is 80° at the DIP joint, 110° at the PIP joint and 90° at the MCP joint. Furthermore, the abduction/adduction angle at the MCP joint has been measured as 20° for the index finger (Bundhoo & Park, 2005).

3. Model of the finger

The finger model of the humanoid robot hand used in this study is considered as a kinematic

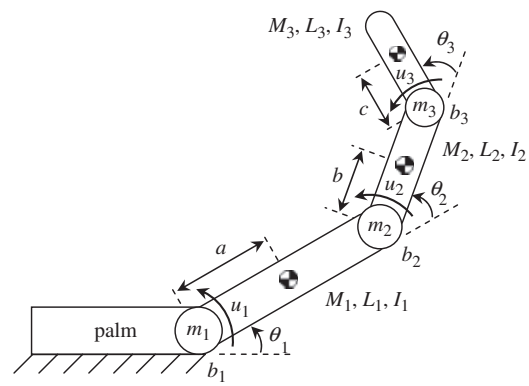

Figure 2: *Finger model of the humanoid robot hand.*

chain having three degrees of freedom. It consists of three cylindrical links, which represent the proximal, middle and distal phalanges of the index finger. Also there are point masses representing the extra weight at articulations at each joint of the finger. The physical model of the finger is given in Figure 2.

M_i, L_i and I_i ($i = 1, 2, 3$) are the mass, link length and mass moment of inertia of the related links. a, b and c are the distances of the mass centre of the first, second and third link,

© 2009 The Authors. Journal Compilation © 2009 Blackwell Publishing Ltd

Table 1: *The numerical parameters for the finger model*

Parameter	*Numerical value*	*Unit*	*Parameter*	*Numerical value*	*Unit*
m_1	0.0027	[kg]	I_2	3.3003×10^{-8}	[kg]
m_2	0.0013	[kg]	I_3	1.0181×10^{-8}	[kg]
m_3	0.0005	[kg]	L_1	0.037	[kg m^2]
$b_1 = b_2 = b_3$	0.0001	[N m s]	L_2	0.019	[kg m^2]
M_1	0.0027	[kg]	L_3	0.017	[kg m^2]
M_2	0.0010	[kg]	a	0.0185	[m]
M_3	0.0004	[kg]	b	0.0095	[m]
I_1	3.1693×10^{-7}	[kg]	c	0.0085	[m]

respectively. m_i represents the mass of the joints and θ_i is the joint angle of the related link. Also, there is viscous friction at each revolute joint denoted by b_i. u_i stands for the control torque acting on the related joint. The link lengths used in this model were determined using camera images of a human hand index finger during its closing motion. Additionally, the diameters of links and joints are based on an x-ray image of a real human hand. Mass values of the links and joints were determined by using a bone density of 1.9 g/cm^3 (Weghe *et al.*, 2004). The parameters for the finger model are tabulated in Table 1.

Equations of motion for the finger model are obtained by using Lagrange equations and are given in state space form as

$$[M(\theta)]\ddot{\theta} + \boldsymbol{C}(\theta, \dot{\theta}) + \boldsymbol{G}(\theta) = \boldsymbol{u} \qquad (1)$$

Here, $[M(\theta)]$ is an $n \times n$ mass matrix of the finger, $\boldsymbol{C}(\theta, \dot{\theta})$ is an $n \times 1$ vector and includes the coriolis and centrifugal terms, $\boldsymbol{G}(\theta)$ is an $n \times 1$ vector of the gravity terms and $\boldsymbol{u}$ is an $n \times 1$ generalized torque vector. For brevity, details of the terms in equation (1) are given in the Appendix. For checking the robust behaviour of the controller, a resistive torque is used at the PIP joint as an unexpected joint friction fault.

4. Controller design

After introducing the sliding mode control in Section 4.1, the proposed fuzzy sliding mode controller for the finger of the humanoid robot hand is presented in Section 4.2.

4.1. Sliding mode control

In sliding mode controlled systems, the control action is deliberately changed during the control process according to certain predefined rules, which depend on the error states of the system. Then, the system moves on stable and unstable trajectories and finally reaches the sliding surface where the error states go to zero by sliding on this surface.

The state space form of a non-linear dynamic system, as in equation (1), can be written as

$$\dot{\boldsymbol{x}} = \boldsymbol{f}(x) + [B]\boldsymbol{u} \qquad (2)$$

Here $\boldsymbol{x}$ is a an $n \times 1$ vector of states, $\boldsymbol{u}$ is an $n \times 1$ control input vector, $\boldsymbol{f}(x)$ is an $n \times 1$ vector and includes the non-linear part of the equations and $[B]$ is an $n \times n$ control input matrix. For a control system, the sliding surface can be selected as

$$\boldsymbol{\sigma} = [G]\boldsymbol{e} \qquad (3)$$

Here $\boldsymbol{e} = \boldsymbol{x}_r - \boldsymbol{x}$ is the difference between the reference value and the system response. $[G]$ includes the sliding surface slopes. Then

$$\sigma_i = \alpha_i e_i + \dot{e}_i \qquad (4)$$

α_i represents the negative value of each related sliding surface slope. For stability, the following Lyapunov function candidate, which is proposed for a non-chattering action, has to be positive definite and its derivative has to be negative semi-definite.

© 2009 The Authors. Journal Compilation © 2009 Blackwell Publishing Ltd

$$v(\boldsymbol{\sigma}) = \frac{\boldsymbol{\sigma}^{\mathrm{T}}\boldsymbol{\sigma}}{2} > 0 \tag{5}$$

$$\frac{\mathrm{d}v(\boldsymbol{\sigma})}{\mathrm{d}t} = \frac{\dot{\boldsymbol{\sigma}}^{\mathrm{T}}\boldsymbol{\sigma}}{2} + \frac{\boldsymbol{\sigma}^{\mathrm{T}}\dot{\boldsymbol{\sigma}}}{2} \leq 0 \tag{6}$$

If the limit condition is applied to equation (6), the controller force for the limit case is obtained from equations (2) and (3).

$$\boldsymbol{u}_{\mathrm{eq}} = [GB]^{-1}\left(\frac{\mathrm{d}\boldsymbol{\Phi}(t)}{\mathrm{d}t} - [G]\boldsymbol{f}(x)\right) \tag{7}$$

Here $\boldsymbol{\Phi}(t) = [G]\boldsymbol{x}_{\mathrm{r}}$. Equivalent control is valid only on the sliding surface. So an additional term should be defined to pull the system to the surface. For this purpose the derivative of the Lyapunov function can be selected as follows.

$$\dot{\boldsymbol{v}} = -\boldsymbol{\sigma}^{\mathrm{T}}[\Gamma]\boldsymbol{\sigma} < 0 \tag{8}$$

By equating equations (6) and (8) and carrying out the necessary calculations, the total control input is found as

$$\boldsymbol{u} = \boldsymbol{u}_{\mathrm{eq}} + [GB]^{-1}[\Gamma]\boldsymbol{\sigma} \tag{9}$$

$[GB]^{-1}$ is always invertible and equal to the mass matrix for mechanical systems. The control gain matrix $[\Gamma]$ is a positive definite matrix and its entries are decided by trial at the design stage. However, if knowledge of $\boldsymbol{f}(x)$ and $[B]$ is not well known, the calculated equivalent control inputs will be completely different from the needed equivalent control inputs. Thus, in this study, it is assumed that the equivalent control is the average of the total control. For estimation of the equivalent control, an averaging filter, here a low pass filter, can be designed as follows.

$$\hat{\boldsymbol{u}}_{\mathrm{eq}} = \frac{1}{\tau s + 1}\boldsymbol{u} \tag{10}$$

Here, τ is the time constant of the low pass filter. Finally the non-chattering control input is defined as

$$\boldsymbol{u} = \hat{\boldsymbol{u}}_{\mathrm{eq}} + [GB]^{-1}[\Gamma]\boldsymbol{\sigma} \tag{11}$$

4.2. *Fuzzy sliding mode control with adaptive control gain*

In this section a fuzzy logic approach for tuning the control gain of the sliding mode controller is presented. The proposed fuzzy logic scheme changes the control gain of the sliding mode controller dynamically using certain heuristic decision rules; thus, an adaptive fuzzy sliding mode controller is obtained.

In the proposed fuzzy logic scheme, the sliding surface σ_i and its derivative $\dot{\sigma}_i$ are used as inputs and the output is the control gain Γ_i of the sliding mode controller. Thus, a fuzzy logic unit with two inputs and a single output is used. For fuzzification of the input and output variables, Gaussian membership functions are used as shown in Figure 3. In this figure, for input membership functions the NB, NS, Z, PS and PB stand for negative big, negative small, zero, positive small and positive big, respectively. Also, for output membership functions the VS, S, M, B and VB stand for very small, small, medium, big and very big, respectively. Input membership functions are defined on the closed interval $[-1, 1]$ and output membership functions are defined on the closed interval

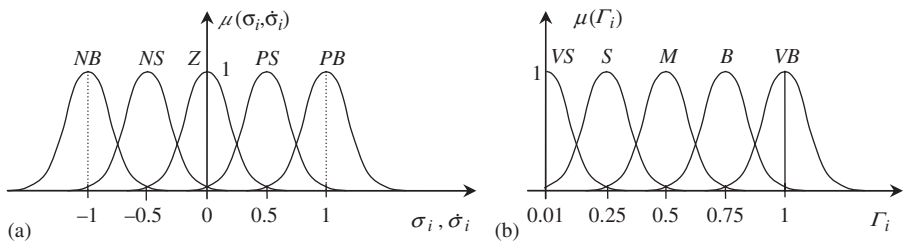

Figure 3: *Membership functions for (a) the input variables and (b) the output variable.*

© 2009 The Authors. Journal Compilation © 2009 Blackwell Publishing Ltd

[0.01, 1], since control gain Γ_i is positive definite as stated in the sliding mode control design. Scaling factors are used in order to map crisp variables into their fuzzy universe of discourse and they are found at the design stage by trial. First, the conventional sliding mode controlled system is simulated, and the bounds of the input variables of the fuzzy logic part of the proposed controller and the bounds of the required output variable for the system are determined. This allows the scaling factors to be tuned by simulating the fuzzy sliding mode controlled system only a few more times before satisfactory results are obtained. The membership function M for the control gain Γ_i is defined in the vicinity of the gain of the conventional sliding mode controller. This allows smaller or larger values for the control gain Γ_i to be obtained whenever necessary.

In order to construct the fuzzy rule base, certain cases are investigated and a few sample rules are discussed below.

If (σ_i: PB) and if ($\dot{\sigma}_i$: Z) then (Γ_i: VB) (case 1)

If (σ_i: PS) and if ($\dot{\sigma}_i$: NB) then (Γ_i: S) (case 2)

If (σ_i: Z) and if ($\dot{\sigma}_i$: PB) then (Γ_i: VS) (case 3)

If (σ_i: Z) and if ($\dot{\sigma}_i$: Z) then (Γ_i: M) (case 4)

Suppose that the system is far from the sliding surface and reaching velocity to the surface is approximately zero, i.e. σ_i is PB and $\dot{\sigma}_i$ is Z. Then, the control gain is selected to be VB in order to bring the system states to the sliding surface rapidly (case 1, Figure 4). In case 2, σ_i is PS and $\dot{\sigma}_i$ is NB, i.e. the system is not far from the sliding surface and it is approaching the surface; thus small control gain is enough and Γ_i is selected to be S. In case 3, the system is on the sliding surface but it tends to leave the surface due to the non-zero sliding function derivative; thus Γ_i is selected to be VS in order to avoid overshoot. In case 4, both σ_i and $\dot{\sigma}_i$ are zero, i.e. the system is on the sliding surface and it cannot leave the surface since the derivative of the sliding surface is zero. Thus, Γ_i is selected to be M as it is for the conventional sliding mode controller. By using similar reasoning the rule base for the fuzzy logic sliding mode controller

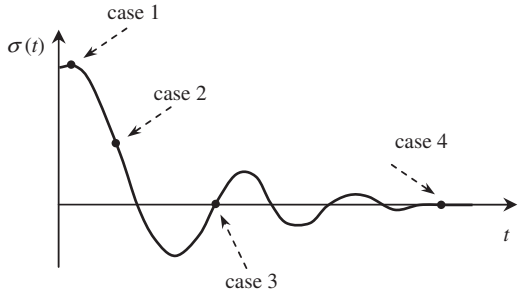

Figure 4: *Graphical representation for the sample rules.*

Table 2: *Decision rules for the control gain*

σ_i	$\dot{\sigma}_i$				
	NB	*NS*	*Z*	*PS*	*PB*
NB	M	B	VB	B	M
NS	S	M	B	M	S
Z	VS	S	M	S	VS
PS	S	M	B	M	S
PB	M	B	VB	B	M

Table 3: *The numerical parameters of the controller*

$SF_{\sigma_1} = 1$	$SF_{\Gamma_1} = 800$
$SF_{\sigma_2} = 0.588$	$SF_{\Gamma_2} = 1400$
$SF_{\sigma_3} = 0.588$	$SF_{\Gamma_3} = 1800$
$SF_{\dot{\sigma}_1} = 0.0025$	$\alpha_i = 1$
$SF_{\dot{\sigma}_2} = 0.00025$	$\tau_i = 0.002$
$SF_{\dot{\sigma}_3} = 0.0004$	

$i = 1, 2, 3$.

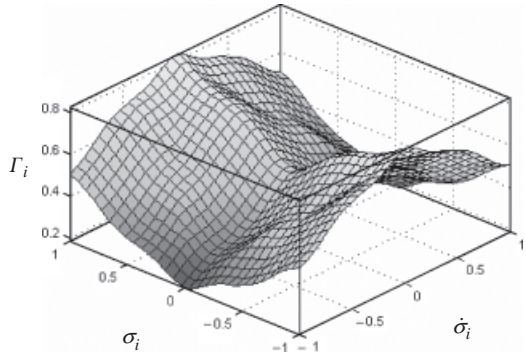

Figure 5: *Fuzzy rule surface.*

© 2009 The Authors. Journal Compilation © 2009 Blackwell Publishing Ltd

with adaptive control gain is constructed; it is given in Table 2.

Numerical parameters for the proposed fuzzy sliding mode controller are given in Table 3. SF_{σ_i} and $SF_{\dot{\sigma}_i}$ are the input scaling factors and SF_{Γ_i} is the output scaling factor of the fuzzy logic unit.

Figure 5 depicts the rule surface for the fuzzy adaptation part of the proposed fuzzy sliding mode controller. The block diagram, illustrating the system and controller structure, is presented in Figure 6.

5. Trajectory planning and numerical results

Since the humanoid robot finger is expected to simulate the natural movement of the human

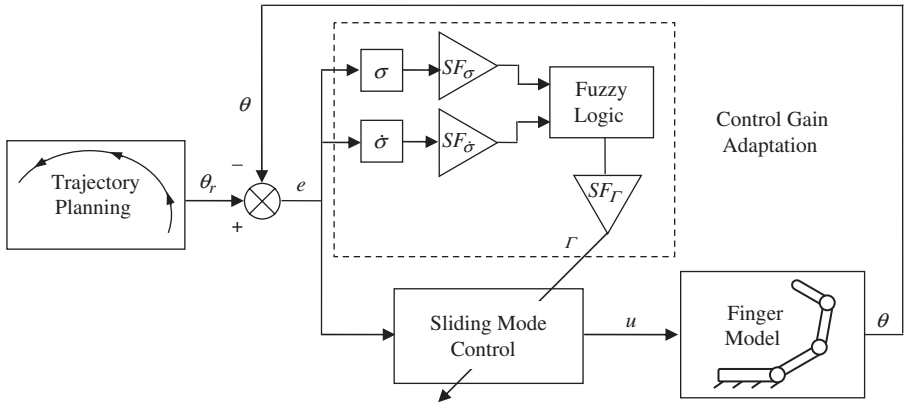

Figure 6: *The system and controller structure.*

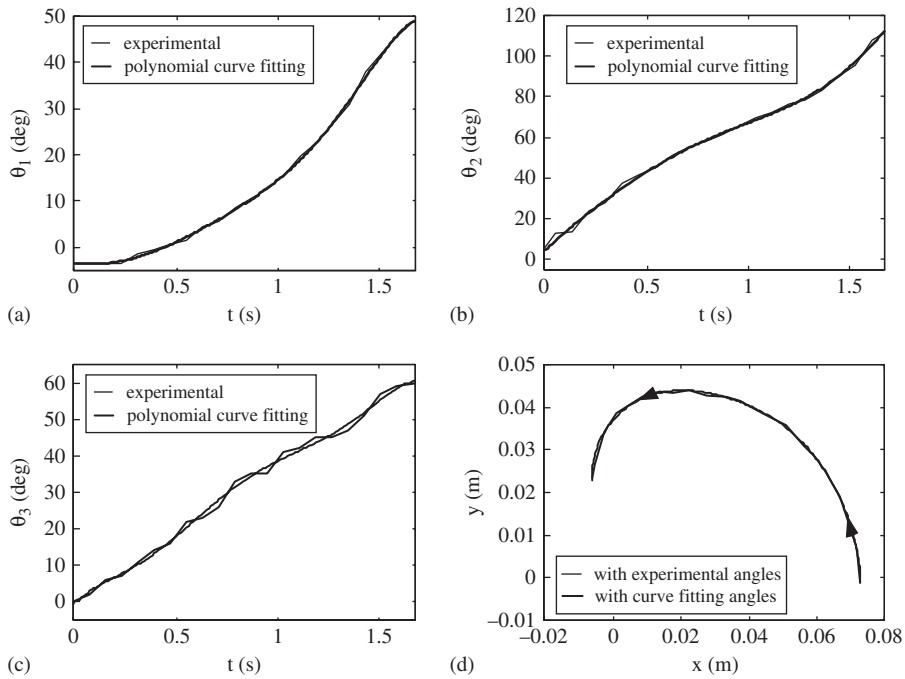

Figure 7: *(a), (b), (c) Experimental data of joint angles and their polynomial approximations; (d) trajectory of the robot finger for closing motion.*

© 2009 The Authors. Journal Compilation © 2009 Blackwell Publishing Ltd

finger, trajectory planning plays an important role in design. In this study, the flexion movement of the index finger of the human hand is investigated. For this purpose, while the index finger was closing down, the movement of the finger was recorded using a digital camera. The recorded video was split into frames with 0.08 s time intervals. Then, these frames were transferred into a computer-aided design program where the joint angles were measured with the aid of marks previously placed on the finger joints.

In order to have continuous reference paths for the joint angles, sixth-order polynomials were fitted to the experimental data. The data and their polynomial approximations are given in Figures 7(a), 7(b) and 7(c). By using the polynomials as reference, the motion of the end of the distal link is obtained as shown in Figure 7(d). It is seen from this figure that the trajectory obtained is a natural one. Thus, the polynomials will be used as reference for the fuzzy sliding mode controller through the numerical analysis of the finger model.

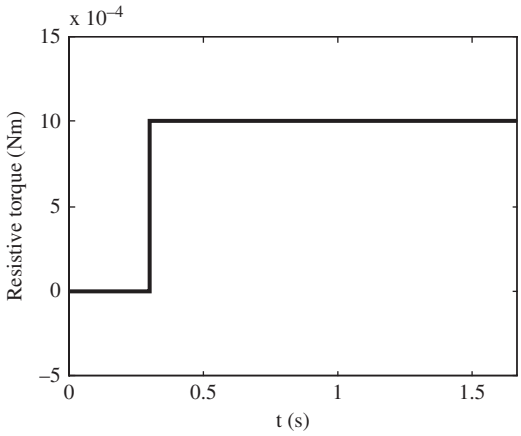

Figure 8: *Applied resistive torque to the PIP joint.*

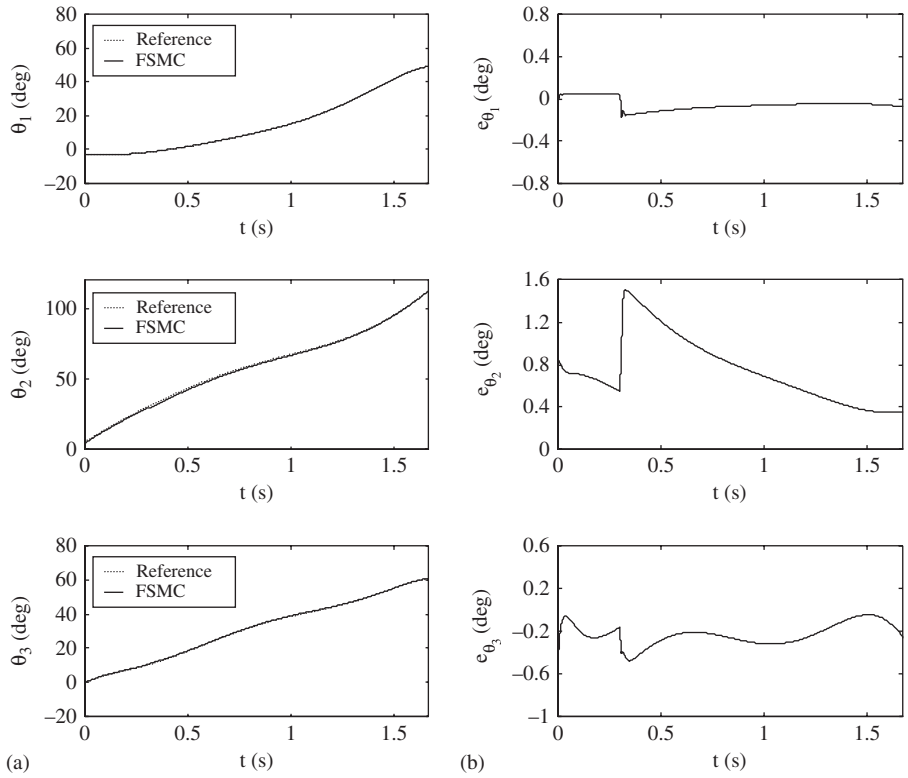

Figure 9: *(a) Reference and actual values for joint angles; (b) tracking errors for the links.*

© 2009 The Authors. Journal Compilation © 2009 Blackwell Publishing Ltd

It should be noted that during simulations an unexpected joint friction fault occurs after 0.3 s, which tests the robust behaviour of the controller. This resistive friction is shown in Figure 8.

Figure 9 gives the reference and actual joint angles and the tracking errors for the related links. It is seen from this figure that tracking errors for the related links are acceptably small and each link of the finger tracks the specified trajectory successfully in spite of the unexpected joint friction fault. This indicates the efficiency and robust behaviour of the proposed fuzzy sliding mode controller.

The control torque input for each link is given in Figure 10. They are the output signals of the controller, and are used to manipulate the finger. The maximum joint torque is obtained for the MCP joint and the minimum torque is obtained for the DIP joint, which are also as expected.

Figure 11 presents a comparison of the related joint angle errors for the conventional sliding mode controller and the proposed fuzzy sliding mode controller. The parameters of the conventional sliding mode controller are determined as $\alpha_i = 1$, $\tau_i = 0.002$, $\Gamma_1 = 200$, $\Gamma_2 = 400$, $\Gamma_3 = 600$. It is observed from this figure that the magnitudes of the related joint angle errors are smaller for the proposed fuzzy sliding mode controller than for the conventional sliding mode controller. Additionally, it is seen that the proposed fuzzy sliding mode controller recovers faster than its conventional counterpart when an unexpected joint friction fault occurs on the PIP joint after 0.3 s.

In order to verify the performance of the proposed controller, two different performance indices are calculated and presented in Table 4, for both the conventional sliding mode control-

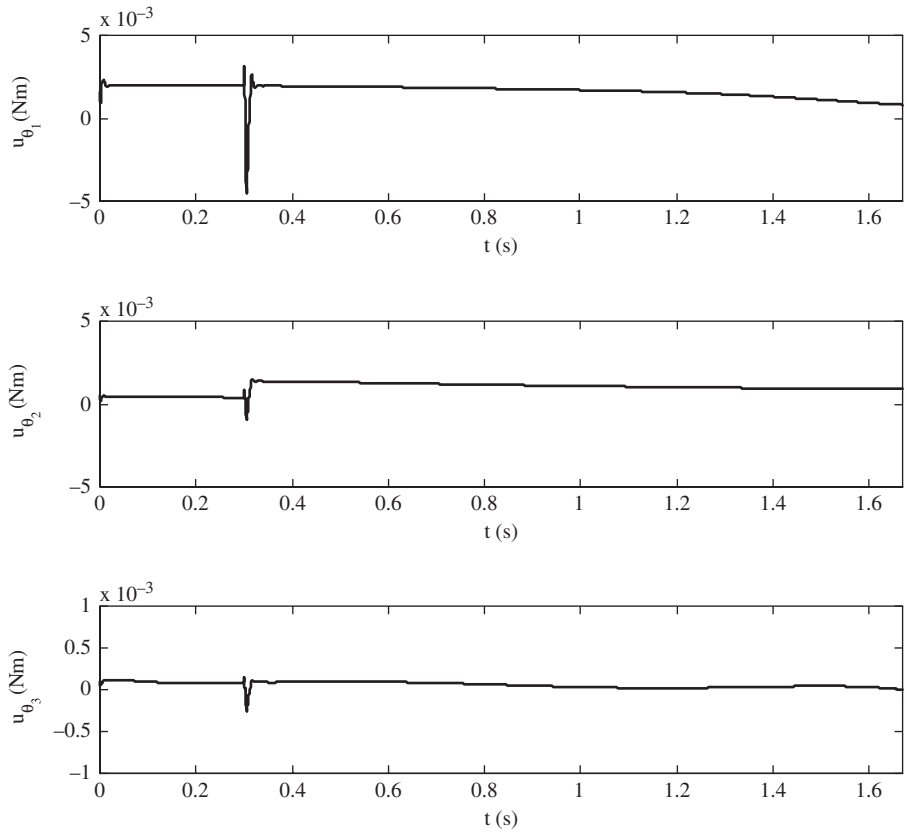

Figure 10: *Control torque inputs produced by the fuzzy sliding mode controller.*

© 2009 The Authors. Journal Compilation © 2009 Blackwell Publishing Ltd

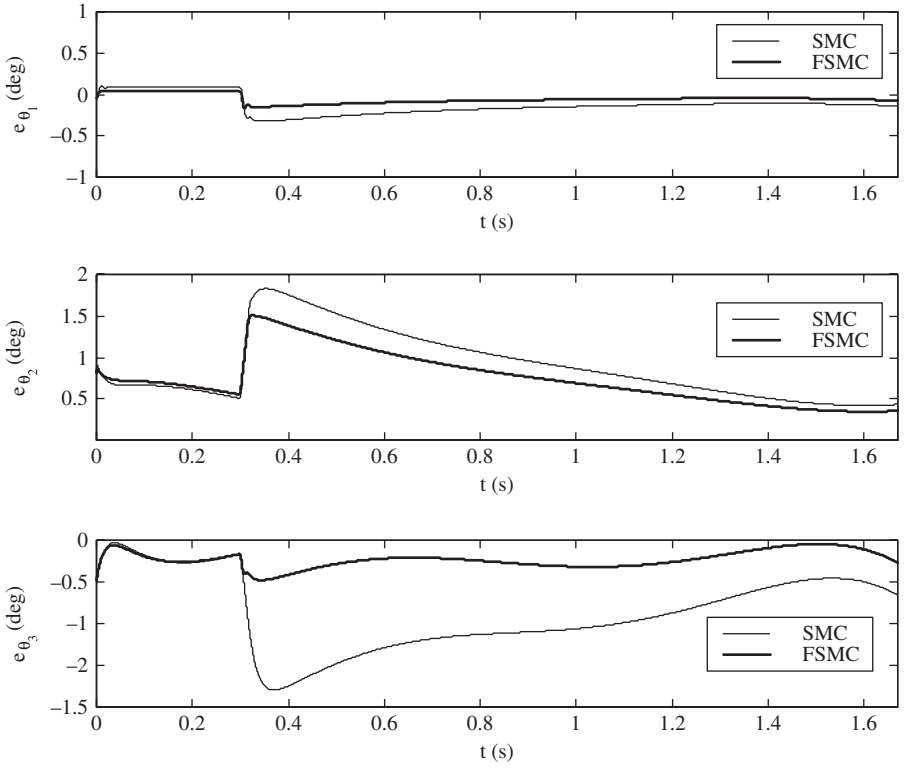

Figure 11: *Comparison of the related joint angle errors for a conventional sliding mode controller (SMC) and the proposed fuzzy sliding mode controller (FSMC).*

Table 4: *Performance indices for the designed controllers*

	MCP joint		*PIP joint*		*DIP joint*	
	IAE $(e_{\theta_1}) \times 10^{-2}$	*ITAE* $(e_{\theta_1}) \times 10^{-2}$	*IAE* $(e_{\theta_2}) \times 10^{-2}$	*ITAE* $(e_{\theta_2}) \times 10^{-2}$	*IAE* $(e_{\theta_3}) \times 10^{-2}$	*ITAE* $(e_{\theta_3}) \times 10^{-2}$
SMC	0.46	0.36	2.60	1.89	2.52	2.07
FSMC	0.20	0.16	2.17	1.53	0.68	0.51

SMC, sliding mode controller; FSMC, fuzzy sliding mode controller.
$i = 1, 2, 3$.

ler and the proposed fuzzy sliding mode controller. The first is the integral of the absolute error (IAE) criterion which penalizes the errors with different signs equally, and the second is the integral of the time multiplied absolute error (ITAE) criterion which penalizes the errors late in time heavily. When the results are investigated it is verified that the proposed fuzzy sliding mode controller outperforms the conventional sliding mode controller since all performance indices for the related joints are smaller for the proposed controller.

6. Conclusion

In this paper, the motion control problem of a humanoid robot hand finger model was investigated. The model design was based on the

 © 2009 The Authors. Journal Compilation © 2009 Blackwell Publishing Ltd

biomechanical features of the human hand index finger. The trajectory of the end point of the finger was determined using camera images during the closing motion of the index finger, and joint angles were obtained with the aid of a computer-aided design program. The equations of motion were acquired by dynamic analysis of the finger model. Then, a robust sliding mode controller improved by a fuzzy logic unit was presented and applied to the system. From the numerical results it is concluded that by using the proposed fuzzy sliding mode controller an efficient tracking performance was obtained despite an unexpected friction fault. Also it was verified that the performance of the proposed fuzzy sliding mode controller is superior to the conventional sliding mode controller since the IAE and ITAE performance index values were reduced. Consequently, the results have shown that the proposed fuzzy sliding mode control technique is preferable for use in humanoid robot hand design in order to improve the life quality of people with amputations.

Appendix

The mass matrix, coriolis–centrifugal vector and gravity vector of the motion equations are as follows:

$$[M(\theta)]=\begin{bmatrix} A_1+A_2+A_3+2L_1A_4c_2+2cM_3(L_1c_{23}+L_2c_3) & A_2+A_3+L_1A_4c_2+cM_3(L_1c_{23}+2L_2c_3) & A_3+cM_3(L_1c_{23}+L_2c_3) \\ A_2+A_3+L_1A_4c_2+cM_3(L_1c_{23}+2L_2c_3) & A_2+A_3+2cM_3L_2c_3 & A_3+cM_3L_2c_3 \\ A_3+cM_3(L_1c_{23}+L_2c_3) & A_3+cM_3L_2c_3 & A_3 \end{bmatrix}$$

$$\boldsymbol{C}(\theta,\dot{\theta})=\begin{bmatrix} b_1\dot{\theta}_1-L_1(A_4s_2+cM_3s_{23})\left(2\dot{\theta}_1\dot{\theta}_2+\dot{\theta}_2^2\right)-cM_3(L_1s_{23}+L_2s_3)\left(2\dot{\theta}_1\dot{\theta}_3+2\dot{\theta}_2\dot{\theta}_3+\dot{\theta}_3^2\right) \\ b_2\dot{\theta}_2+\mu\text{sign}(\dot{\theta}_2)+L_1(A_4s_2+cM_3s_{23})\dot{\theta}_1^2-cM_3L_2s_3\left(2\dot{\theta}_1\dot{\theta}_3+2\dot{\theta}_2\dot{\theta}_3+\dot{\theta}_3^2\right) \\ b_3\dot{\theta}_3+cM_3\left((L_1s_{23}+L_2s_3)\dot{\theta}_1^2+L_2s_3\left(2\dot{\theta}_1\dot{\theta}_2+\dot{\theta}_2^2\right)\right) \end{bmatrix}$$

$$\boldsymbol{G}(\theta)=\begin{bmatrix} g(A_5c_1+A_6c_{12}+cM_3c_{123}) \\ g(A_6c_{12}+cM_3c_{123}) \\ gcM_3c_{123} \end{bmatrix}$$

where

$$A_1=M_1a^2+I_1+(M_2+M_3+m_2+m_3)L_1^2$$

$$A_2=M_2b^2+I_2+(M_3+m_3)L_2^2$$

$$A_3=M_3c^2+I_3$$

$$A_4=M_2b+(M_3+m_3)L_2$$

$$A_5=M_1a+(M_2+M_3+m_2+m_3)L_1$$

$$A_6=M_2b+(M_3+m_3)L_2$$

In the expressions above, the abbreviations $c_1=\cos\ \theta_1$, $s_2=\sin\ \theta_2$, $c_{123}=\cos(\theta_1+\theta_2+\theta_3)$ and $s_{23}=\sin(\theta_2+\theta_3)$ are used.

© 2009 The Authors. Journal Compilation © 2009 Blackwell Publishing Ltd

References

AN, K.N., E.Y. CHAO, W.P. COONEY and R.L. LINSCHEID (1979) Normative model of human hand for biomechanical analysis, *Journal of Biomechanics*, **12** (10), 775–788.

ARMSTRONG, T.J. and D.B. CHAFFIN (1978) An investigation of the relationship between displacements of the finger and wrist joints and the extrinsic finger flexor tendons, *Journal of Biomechanics*, **11** (3), 119–128.

BANKS, J.L. (2001) Design and control of an anthropomorphic robotic finger with multi-point tactile sensation. *MIT AI Lab Technical Report AITR-2001-005*.

BARTOSZEWICZ, A. (1995) A comment on a time-varying sliding surface for fast and robust tracking control of second-order uncertain systems, *Automatica*, **31** (12), 1893–1895.

BIGGS, J. and K. HORCH (1999) A three-dimensional kinematic model of the human long finger and muscles that actuate it, *Medical Engineering and Physics*, **21**, 625–639.

BROOK, N., J. MIZRAHI, M. SHOHAM and J. DAYAN (1995) A biomechanical model of index finger dynamics, *Medical Engineering and Physics*, **17** (1), 54–63.

BUCHHOLZ, B. and T.J. ARMSTRONG (1992) A kinematic model of the human hand to evaluate its prehensile capabilities, *Journal of Biomechanics*, **25** (2), 149–162.

BUCHNER, H.J., M.J. HINES and H.A. HEMAMI (1988) Dynamic model for finger interphalangeal coordination, *Journal of Biomechanics*, **21** (6), 459–468.

BUNDHOO, V. and E.J. PARK (2005) Design of an artificial muscle actuated finger towards biomimetic prosthetic hands, *Proceedings of the 12th International Conference on Advanced Robotics, Seattle*, New York: IEEE Press, 368–375.

DE CAMPOS, T.E. (2006) 3D hand and object tracking for intention recognition, PhD Thesis, Oxford University.

CAVALLO, A. and C. NATALE (2004) High-order sliding control of mechanical systems: theory and experiments, *Control Engineering Practice*, **12**, 1139–1149.

CHOI, S.B., C.C. CHEONG and D.W. PARK (1993) Moving switching surfaces for robust control of second-order variable structure systems, *International Journal of Control*, **58** (1), 229–245.

GAO, W. and J.C. HUNG (1993) Variable structure control of nonlinear systems: a new approach, *IEEE Transactions on Industrial Electronics*, **40** (1), 45–55.

GRAY, H. (1858) *Gray's Anatomy: Descriptive and Surgical*, http://en.wikipedia.org/wiki/Grays_Anatomy; last accessed 25 May 2006.

GUO, Y. and P.Y. WOO (2003) Adaptive fuzzy sliding mode control for robotic manipulators, *Proceedings of the 42nd IEEE Conference on Decision and Control*, New York: IEEE Press, 2174–2179.

HA, Q.P., D.C. RYE and H.F.D. WHYTE (1999) Fuzzy moving sliding mode control with application to robotic manipulators, *Automatica*, **35** (4), 607–616.

HERMAN, P. (2005) Sliding mode control of manipulators using first-order equations of motion with diagonal mass matrix, *Journal of the Franklin Institute*, **342**, 353–363.

HIRZINGER, G., J. BUTTERFASS, M. FISCHER, M. GREBENSTEIN, M. HAHNLE, H. LIU, I. SCHAEFER and N. SPORER (2000) A mechatronics approach to the design of light-weight arms and multifingered hands, *Proceedings of the IEEE International Conference on Robotics and Automation*, New York: IEEE Press, 46–54.

JACOBSEN, S., E. IVERSEN, D. KNUTTI, R. JOHNSON and K. BIGGERS (1986) Design of the Utah/MIT dextrous hand, *Proceedings of the IEEE International Conference on Robotics and Automation*, New York: IEEE Press, 1520–1532.

KAZEMIAN, H.B. (2005) Developments of fuzzy PID controllers, *Expert Systems*, **22** (5), 254–264.

LAVIOLA, J.J. Jr (1999) A survey of hand posture and gesture recognition techniques and technology, *Technical Report CS-99-11*, Department of Computer Science, Brown University.

LI, Z.M., V.M. ZATSIORSKY and M.L. LATASH (2000) The effect of extensor mechanism on finger flexor force, 24th Annual Meeting of the American Society of Biomechanics, University of Illinois at Chicago, 19–22 July.

LIN, C.M. and Y.J. MON (2003) Hybrid adaptive fuzzy controllers with application to robotic systems, *Fuzzy Sets and Systems*, **139**, 151–165.

MILLER, A., P. ALLEN, V. SANTOS and F. VALERO-CUEVAS (2005) From robotic hands to human hands: a visualization and simulation engine for grasping research, *Industrial Robot*, **32** (1), 55–63.

POLLARD, N. and R.C. GILBERT (2002) Tendon arrangement and muscle force requirements for humanlike force capabilities in a robotic finger, *Proceedings of the IEEE International Conference on Robotics and Automation*, New York: IEEE Press, 3755–3762.

SLOTINE, J.J. and S.S. SASTRY (1983) Tracking control of nonlinear systems using sliding surfaces, with application to robot manipulators, *International Journal of Control*, **38** (2), 465–492.

TOKAT, S. (2006) Time-varying sliding surface design with support vector machine based initial condition adaptation, *Journal of Vibration and Control*, **12** (8), 901–926.

UTKIN, V.I. (1977) Variable structure systems with sliding modes, *IEEE Transactions on Automatic Control*, **22**, 212–222.

 © 2009 The Authors. Journal Compilation © 2009 Blackwell Publishing Ltd

VALERO-CUEVAS, F.J. (2005) An integrative approach to the biomechanical function and neuromuscular control of the fingers, *Journal of Biomechanics*, **38**, 673–684.

VIGOUROUX, L., F. QUAINE, A. LABARRE-VILA and F. MOUTET (2006) Estimation of finger muscle tendon tensions and pulley forces during specific sport-climbing grip techniques, *Journal of Biomechanics*, **39**, 2583–2592.

WEGHE, M.V., M. ROGERS, M. WEISSERT and Y. MATSUOKA (2004) The ACT hand: design of the skeletal structure, in *Proceedings of the IEEE International Conference on Robotics and Automation*, New York: IEEE Press, 3375–3379.

YOUM, Y., T.E. GILLESPIE, A.E. FLATT and B.L. SPRAGUE (1978) Kinematic investigation of normal MCP joint, *Journal of Biomechanics*, **11** (3), 109–118.

The authors

Yunus Ziya Arslan

Yunus Ziya Arslan received the BS degree in 2002 and MS degree in 2005 both from the Department of Mechanical Engineering of Istanbul University. He is currently a PhD student and research assistant in the Department of Mechanical Engineering of Istanbul University and visiting student at the University of Calgary. His research areas include biomechanics of the musculoskeletal systems, and modelling and control of robotic manipulators.

Yuksel Hacioglu

Yuksel Hacioglu received the BS degree in 2002 and MS degree in 2004 both from the Department of Mechanical Engineering of Istanbul University. He is currently a PhD student and research assistant in the Department of Mechanical Engineering of Istanbul University. His research areas include modelling and control of robotic manipulators, modelling and control of vehicle systems, non-linear control theory and fuzzy logic.

Nurkan Yagiz

Nurkan Yagiz is currently a Professor in the Mechanical Engineering Department of Istanbul University. He received the BS degree in 1984 and MS degree in 1986 from the Department of Mechanical Engineering of the Middle East Technical University in Ankara and the PhD degree from the Department of Mechanical Engineering of Istanbul University in 1993. His research areas include modelling and control of vehicle systems, control of structural vibrations and non-linear control theory.

© 2009 The Authors. Journal Compilation © 2009 Blackwell Publishing Ltd